Program Digest, 2019 IEEE International Ultrasonics Symposium (IUS)
Glasgow, Scotland, October 6-9, 2019

Flowline tracking Doppler

Stefano Fiorentini*†, Ingvild Kinn Ekroll*†§, Hans Torp*†, Jørgen Avdal*†
*Department of Circulation and Medical Imaging, Norwegian University of Science and Technology, Trondheim, Norway
†Center for Innovative Ultrasound Solutions, Trondheim, Norway
Kirurgisk klinikk, St. Olavs Hospital, Trondheim, Norway
Email: stefano.fiorentini@ntnu.no

***Abstract*—Transit-time broadening in regions with high blood velocities limits the reproducibility of measurements from Pulsed Wave (PW) Doppler, which is a standard diagnostic tool in several cardiovascular applications. 2-D tracking Doppler, a previously introduced spectral estimator, can reduce transit time broadening by following the blood scatterers along straight trajectories. However, this method is expected to provide limited benefits in case of curved flow trajectories. In this work, we extended the 2-D tracking Doppler spectral estimator to track along arbitrarily shaped trajectories. Results from simulations showed that the extended implementation, named flowline tracking Doppler, delivers sonograms with improved velocity resolution compared to the previous implementation in case of curved flow trajectories. Results were confirmed using *in vitro* recordings.**

I. Introduction

In conventional pulsed wave (PW) Doppler, the velocity distribution within the sample volume is estimated from the periodogram of the of the backscattered signal from consecutive pulses. Because the reflectors remain within the insonified sample volume for a limited amount of time, the resulting Doppler spectrum will be affected by spectral broadening even under the ideal case of a uniform velocity profile and long observation windows. This phenomenon is known as transit-time broadening and has been extensively investigated in the literature [1], [2]. Spectral broadening is a major challenge in spectral flow estimation because it limits the reproducibility of measurements and leads to velocity overestimation.

Several methods have been proposed to reduce spectral broadening. Adaptive spectral estimators such as the Capon spectral estimation and the Amplitude and Phase estimator can improve spectral resolution at short ensemble lengths [3], [4], however they don't succeed at reducing transit-time broadening. In 2-D tracking Doppler [5] a velocity spectrum with reduced transit-time broadening is estimated by following the reflectors along user defined straight trajectories in order to extend the observation window. However, there are several cases in which the flow trajectory is not necessarily straight. Carotid bifurcation, umbilical cord and aortic arch are a few examples in which curved flow patterns may occur. Using a straight tracking trajectory in the aforementioned applications would be a suboptimal choice, because it would approximate the true flow trajectory only for short lengths, resulting in a limited increase in the observation window.

In this work, we extend the 2-D tracking Doppler estimator to track the blood scatterers along arbitrary curved trajectories. The new implementation is expected to perform better in cases in which the curvature radius of the flow trajectory is comparable to the tracking length. The performance of the extended tracking Doppler spectral estimator is investigated using simulated ultrasound data and recordings from a flow phantom. Finally, our proposed method is compared against both conventional PW Doppler and the previous tracking Doppler implementation.

TABLE I
Acquisition and post-processing parameters

Parameter	Symbol	Value
Transmit frequency	f_0	5 MHz
Pulse cycles at f_0	N_c	2.5
Pulse Repetition Frequency	PRF	15 kHz
IQ sampling frequency	f_s	4.5 MHz
Demodulation frequency	f_d	5 MHz
High-pass filter		FIR order 150
Filter cut-off	f_c	5 cm/s
Window size	N_d	150 samples
Tracking length	l_t	2 cm
PW averaging length	l_a	4 mm

II. Methods

A. Algorithm

In our proposed algorithm, a full velocity spectrum is estimated from IQ beamformed data $s_{\text{IQ}}(\vec{x}, k)$, where $\vec{x}$ defines the spatial coordinates and k is the frame index. The process is repeated for every velocity of interest and is accomplished in two steps. First, a packet of $2N + 1$ points is sampled in space along a trajectory that is defined using a parametric function $[f_{\text{x}}(t), f_{\text{z}}(t)] = \vec{f}(t)$. The procedure is repeated for every frame. The sample position along the trajectory is found by computing the arc length along the parametric curve

$$\frac{n\,v}{\text{PRF}} = \int_0^{t_{\text{n}}} \sqrt{\left(\frac{\partial}{\partial t} f_{\text{x}}(t)\right)^2 + \left(\frac{\partial}{\partial t} f_{\text{z}}(t)\right)^2}\,\text{d}t \qquad (1)$$

where v is the velocity of interest $n \in [-N, N]$ is the sample index within the packet and PRF is is the Pulse Repetition Frequency. Equation 1 can be solved numerically to estimate the parameter t_{n}, which is used to estimate the samples coordinates $\vec{x}(v, n) = \vec{f}(t_{\text{n}})$. The signal $s_{\text{IQ}}(\vec{x}(v, n), k)$ is obtained using spatial interpolation.

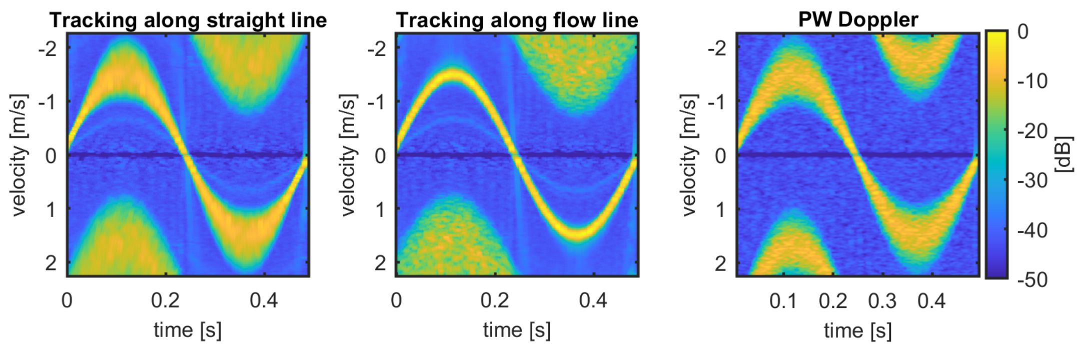

Figure 1. Tracking Doppler and PW Doppler spectra generated from the simulated flow phantom shown in Figure 2. The tracking Doppler spectra were estimated along the 2 cm long straight and curved trajectories shown in the picture. The PW Doppler sample volume was placed at the middle of the tracking trajectories.

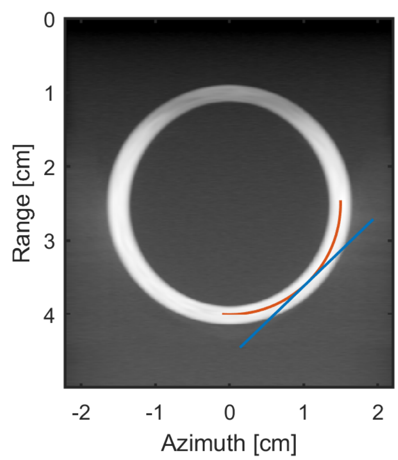

Figure 2. Power Doppler processed from simulated ultrasound data of a flow phantom.

The spectral power $P(v,k)$ is estimated in a second step by squaring the sum of samples within each packet.

$$P(v,k) = \left| \sum_{n=-N}^{N} w(n) \hat{s}(\vec{x}(v,n), k+n) \right|^2 \tag{2}$$

where $n \in [-N, N]$ is the sample index within the packet. A window function $w(n)$ of length $2N+1$ is also applied to reduce sidelobes in the spectrum. A phase correction term must be applied before summation to account for radial motion

$$\hat{s}(\vec{x}(v,n), k) = s_{\mathrm{IQ}}(\vec{x}(v,n), k) e^{i4\pi f_{\mathrm{d}} \vec{x}(v,n) \cdot \vec{a}/c_0} \tag{3}$$

where f_{d} is the demodulation frequency, c_0 is the speed of sound and $\vec{a}$ is a unit vector that defines the transmit beam direction.

B. *In silico validation*

Synthetic ultrasound RF channel data from a flow phantom were generated using Field II. The simulated phantom consisted of a circular tube filled with point reflectors and was imaged using a non compounded plane wave sequence. The tube mean radius and diameter were $1.5\,\mathrm{cm}$ and $2\,\mathrm{mm}$ respectively, and the reflector density was high enough to achieve fully developed speckle. The reflectors moved within the phantom with tangential velocity equal to $v = \omega(t)r$ where $\omega(t)$ is the radial velocity and r is the distance of the reflector from the center of rotation. The radial velocity component $\omega(t)$ was defined as a sinusoidal function with $2\,\mathrm{Hz}$ frequency and $100\,\mathrm{rad/s}$ peak radial velocity, resulting in $1.5\,\mathrm{m/s}$ peak tangential velocity at the mean tube radius. GE 9L transducer geometry and impulse response were used to simulate the ultrasound data. The RF channel data sampling frequency was set to $50\,\mathrm{MHz}$ to prevent aliasing and noise was added to achieve $20\,\mathrm{dB}$ SNR. RF channel data were complex demodulated and down sampled before beamforming. Finally, beamformed data were high pass filtered using a $5\,\mathrm{cm/s}$ cut-off FIR filter. A summary of the acquisition and post processing parameters is given in Table I and a power Doppler depiction of the phantom is given in Figure 2. PW Doppler, linear tracking Doppler and flowline tracking Doppler spectra were generated at the two location indicated in Figure 2. PW Doppler spectra were averaged for $4\,\mathrm{mm}$ along the radial direction. The tracking length was set to $2\,\mathrm{cm}$ for both linear and flowline tracking Doppler, and the tracking trajectories are also highlighted in Figure 2.

C. *In vitro validation*

IQ Channel data from a flow phantom were recorded using a GE E95 ultrasound scanner, equipped with a GE 9L linear probe. The scanner was locally modified to enable non compounded plane wave acquisition. The phantom consisted of a $4\,\mathrm{mm}$ diameter tube, and was shaped to achieve a $1.5\,\mathrm{cm}$ curvature radius. The transducer was manually positioned to prevent out-of-plane flow. Channel data processed offline offline. PW Doppler, linear tracking Doppler and flowline tracking Doppler spectra were generated at the location indicated in Figure 4. PW Doppler spectra were averaged for $4\,\mathrm{mm}$ along the radial direction. The tracking length was set

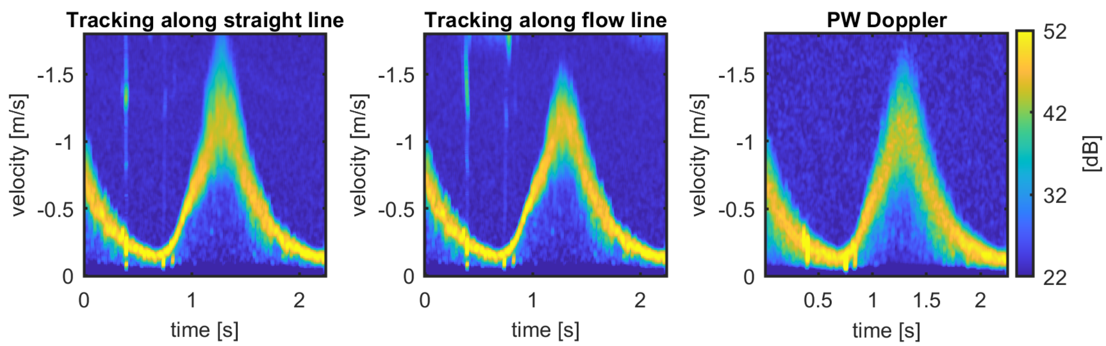

Figure 3. Tracking Doppler and PW Doppler spectra generated from the recorded flow phantom shown in Figure 4. The tracking Doppler spectra were estimated along the $2\,\mathrm{cm}$ long straight and curved trajectories shown in the picture. The PW Doppler sample volume was placed at the middle of the tracking trajectories.

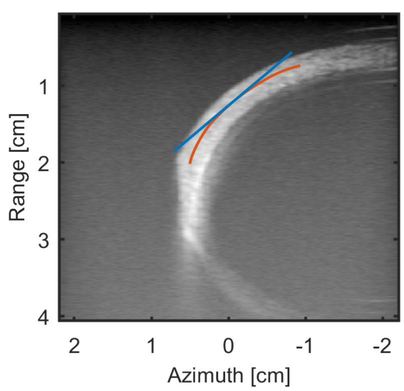

Figure 4. Power Doppler processed from the in vitro recording of a tube phantom.

to $1.8\,\mathrm{cm}$ for both linear and flowline tracking Doppler, whose trajectories are also highlighted in Figure 4.

III. Results

In Figure 1 the spectra generated from simulated ultrasound data of a flow phantom are compared. The PW spectra was generated at the sample point shown in Figure 2. The two trajectories used to generate the tracking Doppler spectra are also shown. The beam-to-flow angle at the PW sample volume was $45°$.

In Figure 3 the spectra generated from the in vitro flow phantom are compared. The PW spectra was generated at the sample point shown in Figure 4. The tracking trajectories used to generate the tracking Doppler spectra are also shown. The curved tracking trajectory was manually defined, and followed the center line of the tube. The beam-to-flow angle at the PW sample volume location was $45°$.

IV. Discussion

In this work we have presented an extension of the 2-D tracking Doppler spectral estimator [5]. The new implementation is capable of generating velocity spectra by tracking the scatterers along arbitrary trajectories, whereas the previous implementation was limited to straight trajectories. The method potentially enables us to extend the tracking length in cases of curved flow, whereas the tracking segment was previously limited to the maximum length in which the tangent could approximate the curved trajectory. It should be noted that the main limitations of tracking Doppler still apply, meaning that the method is still not expected to reduce transit-time broadening in case of turbulent flow or under intense accelerations.

Results in Figure 1 show that, under laminar flow conditions and absence of out-of-plane flow, tracking the blood scatterers along the correct flow trajectory delivers spectra with uniform spectral broadening at all velocities, whereas PW Doppler spectral broadening increases with the scatterer velocity due to transit-time effect. Tracking along a straight line delivers similar performance at low velocities, because the tracking length is short enough to assume the trajectory curvature negligible. However, at higher velocities tracking along a straight line performs similarly to PW Doppler. In fact, for longer tracking lengths the flow curvature is not negligible anymore, resulting in errors in the applied phase correction factor (from Equation 3) and in the scatterers being tracked.

Results from simulations were confirmed by the results from an *in vitro* flow phantom shown in Figure 3. Tracking Doppler performed along the straight and curved trajectories shown in Figure 4 delivered spectra with comparable spectral broadening at low velocities, in which the tracking length was short enough to approximate the curved flow trajectory to its tangent. However, tracking along a straight line delivered increased broadening at higher velocities, due to the increasing difference between the actual flow trajectory and the tangent. It should be noted that, in contrast with simulation results, tracking along the flow trajectory did not generate a spectrum with constant broadening at all velocities, and we identified two possible causes for this discrepancy. First, it was challenging to avoid out-of-plane flow. In fact, it can be seen from Figure 4 that the power Doppler intensity decreases in the lower half of the figure, most likely because of the non complete alignment of the imaging plane with the phantom.

Second, having used water as blood mimicking fluid, we could not avoid the establishment of a turbulent regime at higher velocities and, as previously stated, tracking Doppler is not expected to deliver improved performance under turbulent flow.

The clinical value of this method remains to be investigated. In a preliminary *in vivo* study on a healthy volunteer we investigated whether the proposed method could reduce spectral broadening when estimating blood velocities at the carotid bifurcation. A tracking Doppler velocity spectrum was generated by tracking the blood signal along flowlines estimated from an aliasing-resistant vector Doppler method [6]. Results showed that it was challenging to achieve any improvements by tracking the blood signal along the estimated flowlines rather than tracking the blood signal along the tangent of the flowlines. However, it should be noted that in this study we used a fixed tracking trajectory to generate the velocity spectra from multiple ensembles. Due to the transient nature of the flow field, the validity of any estimated flow trajectory is limited to a stationarity interval of around $10\,\mathrm{ms}$, and improvements may be achieved by updating the tracking trajectory at every ensemble, in a similar fashion to [7]. Moreover, results from fluid flow simulations and recordings using 3-D plane wave sequences [8] revealed that blood flow at the carotid bifurcation exhibits complex three-dimensional patterns and that out-of-plane flow may be challenging to avoid. Further work will investigate the performance of the method in other clinical applications such as blood flow estimation in the umbilical arteries and in the aortic arch.

V. Conclusion

In this work we presented an extension of the 2-D tracking Doppler spectral estimator, which enabled us to track the blood scatterers along arbitrary curved trajectories. Results from simulations and recordings of a flow phantom showed that the new implementation allowed for increasing the tracking length in cases of curved flow. Future work will investigate the in vivo feasibility of the method.

References

[1] V. Newhouse, P. Bendick, and L. Varner, "Analysis of transit time effects on Doppler flow measurement", *IEEE Transactions on Biomedical Engineering*, vol. 23, no. 5, pp. 381–6, 1976.

[2] V. Newhouse, E. Furgason, G. Johnson, and D. Wolf, "The dependence of ultrasound Doppler bandwidth on beam geometry", *IEEE Transactions on Sonics and Ultrasonics*, vol. 27, no. 2, pp. 50–59, 1980.

[3] F. Gran, A. Jakobsson, and J. A. Jensen, "Adaptive spectral Doppler estimation", *IEEE Transactions on Ultrasonics, Ferroelectrics, and Frequency Control*, vol. 56, no. 4, pp. 700–714, Apr. 2009.

[4] I. K. Ekroll, H. Torp, and L. Løvstakken, "Spectral Doppler estimation utilizing 2-D spatial information and adaptive signal processing", *IEEE Transactions on Ultrasonics, Ferroelectrics and Frequency Control*, vol. 59, no. 6, pp. 1182–92, 2012.

[5] T. D. Fredriksen, I. K. Ekroll, L. Løvstakken, and H. Torp, "2-D tracking Doppler: A new method to limit spectral broadening in pulsed wave Doppler", *IEEE Transactions on Ultrasonics, Ferroelectrics and Frequency Control*, vol. 60, no. 9, pp. 1896–905, 2013.

[6] I. K. Ekroll, J. Avdal, A. Swillens, H. Torp, and L. Løvstakken, "An extended least squares method for aliasing-resistant vector velocity estimation", *IEEE transactions on Ultrasonics, Ferroelectrics, and Frequency Control*, vol. 63, no. 11, pp. 1745–1757, 2016.

[7] J. Avdal, L. Løvstakken, H. Torp, and I. K. Ekroll, "Combined 2-D vector velocity imaging and tracking Doppler for improved vascular blood velocity quantification", *IEEE Transactions on Ultrasonics, Ferroelectrics, and Frequency Control*, vol. 64, no. 12, pp. 1795–1804, Dec. 2017.

[8] M. Correia, J. Provost, M. Tanter, and M. Pernot, "4-D ultrafast ultrasound flow imaging: In vivo quantification of arterial volumetric flow rate in a single heartbeat", *Physics in Medicine and Biology*, vol. 61, pp. 48–61, Dec. 2016.